Ice Crystal Production by Mountain Surfaces

DAVID C. ROGERS* AND GABOR VALI

Department of Atmospheric Science, University of Wyoming, Laramie, WY 82071

(Manuscript received 11 October 1986, in final form 11 February 1987)

ABSTRACT

Evidence is presented for a process of ice crystal generation in supercooled orographic clouds in contact with snow-covered mountain surfaces. Comparisons of the crystal concentrations at the surface with aircraft sampling indicate that the "anomalous" crystals originate at the interface of the cloud with the surface. Crystal concentrations at the surface, over the temperature range −5° to −23°C, were found to be roughly 100 times higher than in the main body of the clouds. Occasionally, the effect extends to altitudes as much as 1 km above the ground in the clouds studied, and indications are that even greater depths of clouds might be influenced over extended mountain ranges. The mechanism of ice crystal generation involved has not yet been firmly established; several possibilities are discussed in the paper. The phenomenon can be expected to have significant implications for the characteristics of low-altitude orographic clouds with respect to their propensity to produce precipitation; radiative, chemical and electric properties; and their suitability for cloud seeding.

1. Introduction

Mountain peaks enveloped by clouds have been utilized many times for systematic studies of cloud characteristics and cloud processes [for example: Kohler (1925) in Norway; Langmuir (1948) at Mt. Washington; Kuettner (1950) at Zugspitze; Rittberger (1959) at Mt. Feldberg; Diem (1962) at Jungfraujoch; Hobbs (1969) in the Olympic mountains; Blyth et al. (1980) at the Great Dun Fell; Borys et al. (1983) in the Colorado Rocky Mountains]. The main advantage of such sites, in comparison to aircraft observations, is that it is relatively easy to gather detailed observations in the clouds' interiors over long periods of time, limited only by the lifetime of the clouds or by the time of their passage over the mountain. Observations at mountain peaks have contributed greatly to the development of cloud physics even before the availability of aircraft capable of penetrating clouds, and mountaintop cloud observations continue to usefully complement aircraft observations. Because of the volume of the mountain, and the large interface area with the cloud, there is, of course, the hazard that the mountain introduces unexpected artifacts into the observations, undermining the representativeness of the data for the cloud aloft.

In the process of studying the origins and evolution of ice crystals in a mountain cap cloud, we discovered that the ice content of the cloud was being influenced by "anomalous" ice crystals which appeared to be generated at the surface of the mountain. In this paper we present these findings and discuss their implications.

2. Observational setting and procedures

The studies to be presented were conducted over the past 12 yr in the cap clouds which envelope the upper parts of Elk Mountain, Wyoming (41°37′50″N, 106°31′40″W) in the winter. Elk Mountain is an isolated peak; the summit elevation is at 3.4 km MSL. Other mountains of comparable height are ~100 km away. The broad upwind valley as at ~2.1 km elevation. The mountain is covered with thin coniferous forest from its base to just below the summit. Most snowfall on the mountain is from traveling cyclones, which occur at about weekly intervals in winter. Snowpack is typically 1 m deep by midwinter. Trees and rocks at the upper elevations are covered by wind-packed snow and rime, which can exceed one-half meter in thickness. Wind speeds near mountain top exceed 10 m s^{-1} more than 50% of the time during winter.

Supercooled clouds envelope the mountain on about one-third of the winter days. About half of those clouds can be described as "cap" clouds, i.e., isolated, shallow, wave-like clouds, the other half consisting of clouds of greater depth, and of larger horizontal extent than the mountain. During cap cloud episodes, the cloud top is usually defined by an inversion, equivalent potential temperature is nearly constant from the valley surface to the inversion, snowfall is absent or very light, and rime accumulates on rocks, trees and snowcover. Major characteristics of the cap clouds have been summarized by Rogers and Politovich (1981). The attributes which make the clouds especially suitable for cloud physics studies are smooth, steady and relatively simple flow; stationarity over the mountain; quasi-steady conditions of cloud temperature and horizontal and vertical di-

* Present affiliation: Department of Atmospheric Science, Colorado State University, Fort Collins, CO 80523.

mensions; small vertical lifting (typically less than 1 km); and relatively small temperature range throughout the cloud (typically less than 5°C). The liquid water characteristics of the cap clouds were described in more detail by Politovich and Vali (1983). The origin of ice in the cap clouds has been discussed by Cooper and Vali (1981). Measurements of the electric charges on ice particles in the cap clouds were reported by Saunders (1978).

The major facilities which were used in the Elk Mountain studies are the Elk Mountain Observatory (EMO) and the University of Wyoming's Queen Air research aircraft (N10UW).

The sketch in Fig. 1 depicts a west–east section across the mountain and the cap cloud, and shows typical locations of research aircraft flight tracks. The usual procedure during research flights was to first skim the cloud top, observing temperature, ice concentrations and water content in the upper 50 m of cloud, and then to fly about 30 km upwind of the mountain to perform a sounding in the upwind valley. Thereafter, the aircraft would make a series of cloud penetrations along the wind, and also orthogonal to the wind in the upwind portion of the cloud. As shown in the figure, the upwind (west) side of the cloud often extends 10 to 15 km from the peak, and has a smooth, gradual updraft. The outflow side of the cloud contains strong, sometimes turbulent downdrafts and was usually not penetrated by the aircraft. The nearly conical shape of the mountain allows some air to flow around as well as over it. The north–south extent of the cloud (perpendicular to the cross section of Fig. 1) usually equals the west–east dimension.

The Elk Mountain Observatory is located at the western end of the summit ridge, about 100 m below and 1 km west of the peak. At the EMO, continuous measurements were made of the temperature, wind speed and direction at 7 m elevation AGL. Spot measurements were made of liquid water content (LWC) using either a cloud droplet impaction device or a rime mass accumulation technique (Rogers et al., 1983). The

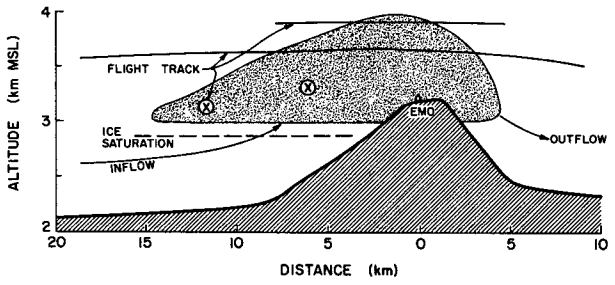

FIG. 1. Cross section along the typical wind direction, showing the profile of Elk Mountain and the outlines of a cap cloud. The location of the Elk Mountain Observatory (EMO) and typical locations of aircraft flight tracks are shown; the circled crosses represent aircraft penetrations orthogonal to the wind.

impaction device also provided information on cloud droplet concentration and size distribution. For some cases, continuous measurements of cloud liquid water were obtained with an Axially Scattering Spectrometer Probe (ASSP, Particle Measuring Systems, Inc., Boulder, Colorado), which was mounted in a wind tunnel. Ice crystal samples were taken from a platform 4 m above the snow surface and about 30 m from the nearest trees. Ice crystals were sampled by impaction onto oil-coated slides (2.5 cm wide) in the wind tunnel (23 m s^{-1} airspeed), or at the end of a rotating arm device (7.5 m s^{-1} speed). The slides were subsequently photographed at 12× magnification while immersed in hexane to avoid evaporation. The theoretical collection efficiency (Ranz and Wong, 1952) of the slides for solid, spherical ice particles becomes <0.5 for sizes below 20 μm diameter with the rotating arm collector and for sizes below 10 μm in the wind tunnel; the collection efficiency is >0.7 for particles above 30 μm. Few crystals < 30 μm were ever observed on the slides and so no corrections for collection efficiency were applied to the data. Therefore, the reported ice crystal concentrations (ICC) probably represent underestimates of the total populations. It is important to emphasize that only pristine crystals of recognizable, symmetrical growth habit were counted and sized; irregularly shaped particles, believed to be aged, resuspended snow, were not included. Descriptions of ice crystal habits are given in terms of the classification of Magono and Lee (1966).

To examine the evolution of ICC and crystal size spectra along the mountain surface, sampling was conducted on some occasions from an enclosed over-snow vehicle both upwind and downwind from the EMO. Crystals were impacted onto oil-coated glass slides which were placed in holders with retractable covers, held about 2 m above the surface and exposed to the windflow for periods of a few to tens of seconds. Wind speed was measured simultaneously to obtain the sample volume.

Temperature and mean winds in cap cloud conditions are quite steady for periods of several hours. Short-term fluctuations in cloud composition are typically about factors of two; hence, only changes larger than that could be resolved for time scales of hours. Sampling rates of several measurements per hour were usually employed.

Instrumentation on the research aircraft has been described by Cooper and Saunders (1980). Measurements were taken of temperature, dewpoint, pressure, airspeed, heading and position, horizontal winds, turbulence, cloud water (ASSP and a droplet impaction device), and ice crystals. The crystal collections were made with a decelerator-impactor device and were photographed using the same technique as at the EMO. Continuous recordings of crystal images were made with a Two-Dimensional Optical Array Spectrometer (2D-C, from Particle Measuring Systems).

TABLE 1. Descriptive parameters of case studies.

	18 Feb 1975	15 Dec 1978	31 Jan 1975	20 March 1975 (Medicine Bow Mountains)	9 Jan 1975
			Cloud conditions		
Cloud top alt (km MSL)	3.63	(UNK*)	4.57	4.57	3.54
Cloud top temperature (°C)	−20.5		−25.0	−15.0	−19.4
Cloud base alt (km MSL)	3.05	3.15	(UNK)	3.66	2.68
Cloud base temperature (°C)	−17.5	−11.9		est. −8	−12.8
Vertical stability	stable	(UNK)	stable	embedded convection	embedded convection
EMO temperature (°C)	−18.0	−13.0	−14.0		−16.0
Winds aloft** (deg/m s^{-1})	270/10	(UNK)	270/20	240/30	340/30
EMO surface winds (deg/m s^{-1})	270/25	245/15	260/25		360/5
Average drop diam (μm)	7	12	9	11	9
Max drop diam (μm)	21	23	12	30	23
Max LWC (g m^{-3})	0.11	1.0	0.15	0.8	0.19
			Ice crystals—aloft **		
A/C flight alt (km MSL)	3.3–3.6		4.0–4.8	4.3–4.5	2.7–2.9
Concentration (l^{-1})	2–7	No	2–10, 60–600	0.4–40	0.5–5
Diam (μm)	60–350	Flight	100–250, 80–140	150–400	300–700
Habit	C1h, P1c		S1, C1h (UNK)	(UNK)	P1c
			Ice crystals—surface		
Concentration (l^{-1})	1–10, 300–800	40–460	40–160		1–17
Diam (μm)	120–500, 40–120	60–180	100–250		50–300
Habit	C1h, C1h	P1c	P1b		P1a

* UNK = unknown.
** At A/C flight altitudes.

3. Case studies

a. 18 February 1975

A cap cloud formed over Elk Mountain on this day with no other clouds above or upwind of the mountain. Temperatures in the cloud ranged from −18° to −20°C. The upwind sounding showed that in the lowest 2 km, the airflow was 10 to 15 m s^{-1} and veered from WSW to WNW. During the 90-min study period, the aircraft made ten penetrations of the cloud at altitudes from 3.32 to 3.57 km MSL. All the passes were along north–south lines, approximately orthogonal to the airflow, and all were in the upwind side of the cloud. A description of the aircraft observations for this day has been reported by Cooper and Vali (1981).

The relevant characteristics of the cloud and a summary of crystal observations are given in Table 1. Figure 2 presents a time history of the crystal observations by the aircraft and at the EMO, demonstrating relative uniformity of conditions throughout the period. Crystal concentrations aloft ranged from 0.03 to 7 l^{-1}, with the lowest concentrations observed only within a few hundred meters of the cloud boundaries and just below the cloud top. In the main body of the cloud, concentrations were fairly uniform and ranged between 2 and 7 l^{-1}. From their analysis of this case, Cooper and Vali (1981) concluded that the crystals aloft formed near the inflow edge of the cloud and few, if any, additional crystals were formed inside the cloud during the transport time of about 500 s through the cloud. A photograph of a crystal sample collected by the aircraft is shown in Fig. 3a. The crystal habits were skeletal thick plates (C1h) and broadbranched crystals (P1c).

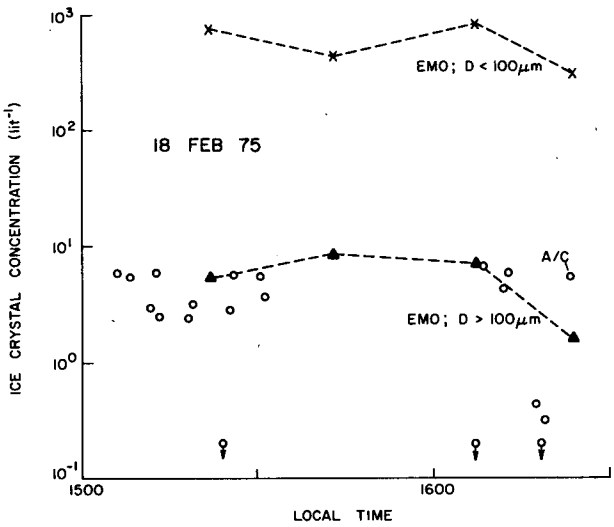

FIG. 2. Ice crystal concentrations observed on 18 February 1975. Circles represent aircraft measurements, while triangles and crosses show the concentrations of large and small crystals at the Elk Mountain Observatory. The concentrations of crystals > 100 μm at the EMO match the concentrations measured aloft; the numbers of small crystals are about 100-times greater.

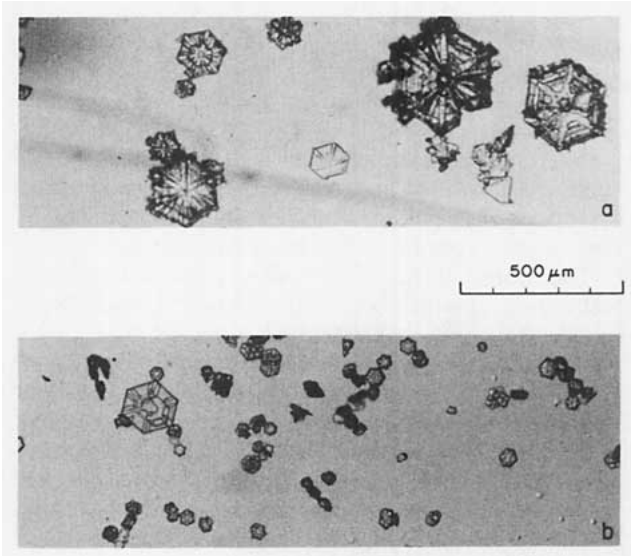

FIG. 3. Selected photographs of ice crystals on 18 February 1975. (a) Aircraft sample: crystal concentration 5.3 per liter, temperature −20.3°C; (b) EMO sample: 800 per liter, −17.9°C. Width of photographs corresponds to 1.9 mm.

Observations at the EMO indicated two distinct populations of ice crystals: a low concentration (1 to 10 l^{-1}) of C1h crystals, 120 to 500 μm in diameter, and a very large concentration (300 to 800 l^{-1}) of much smaller C1h crystals, 40 to 60 μm in diameter. Four samples were collected, at the times indicated in Fig. 2. Size ranges are given so that 60% of the crystal numbers are included. A photograph of crystals collected at the EMO is shown in Figure 3b, and the size distribution for this sample is shown in Figure 4. The high concentration mode in the distribution is at 45 μm and is relatively narrow: the half-width extends from 39 to 63 μm and contains 67% of the total number of crystals.

The concentration, habit and size of the larger crystals (with mode around 150 μm) found at the EMO were in substantial agreement with the observations aloft (cf. Figs. 2 and 3, and Table 1). The high concentration of small crystals was observed only at the surface, suggesting that they had their origins at or near the mountain surface, and that vertical mixing was not sufficient for these small crystals to reach locations sampled by the aircraft.

b. 15 December 1978

Data for this day are from observations at the EMO; no aircraft support was available. The cloud temperature was −13°C, as shown in Table 1, and cloud conditions were fairly steady with respect to both temperature (less than 0.5°C variability over 8 h) and surface winds (variations in mean values were less than 10° and 5 m s^{-1}). Liquid water content averaged about 0.2 g m^{-3}, which corresponds to an adiabatic ascent of about 220 m above cloud base. This is in agreement with the observed cloud base altitude of 3.1 km MSL.

At the EMO, broadbranched crystals (P1c) with mean diameters of about 130 μm were observed in concentrations of 40 to 460 per liter. A photograph of one crystal sample is shown in Fig. 5. Most crystals have the same habit and overall dimensions, indicating similar growth trajectories. Also, most crystals were double structured (Auer, 1971). Many of the centers appeared to be irregularly shaped while others may have been frozen cloud droplets, but this distinction is not unambiguous because it is difficult to be certain that the irregular appearance of some centers is not due to optical distortion or to a lensing effect by oil residue or hexane between the crystal layers. The double structure of P1c and similar crystals is a general observation valid not just for this case. The difficulty of identifying the centers of such crystals is unfortunate, as it means the loss of an important clue to the origins of these crystals. What can be stated with generality is that the centers of double structured crystals are in the size range 10 to 50 μm. Crystals sampled at a given time have the same habit and similar overall dimensions, indicating comparable growth histories.

Ice crystal measurements taken at various points along the mountain surface are summarized in Fig. 6. The sampling locations lay along a WNW line, at an angle of about 30° to the wind direction; locations directly along the wind were inaccessible. Sampling extended over a 2 h time period, but there were no substantial changes in cloud conditions during that time.

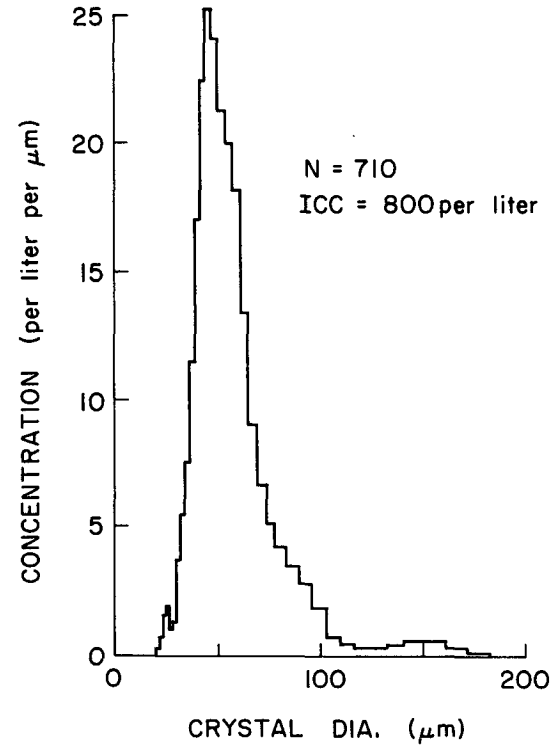

FIG. 4. Size distribution of the ice crystal sample shown in Fig. 3b, collected at the EMO on 18 February 1975.

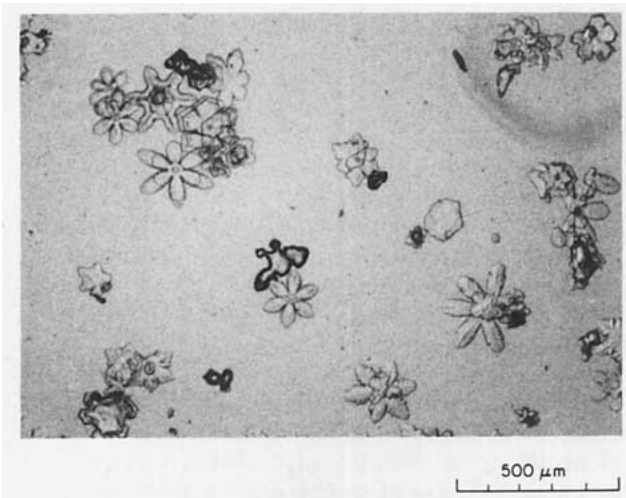

FIG. 5. Ice crystal sample collected at the EMO on 15 December 1978 at a temperature of −13.1°C. The crystal concentration is 148 per liter. Width of photograph corresponds to 1.9 mm.

The sequence of crystal samples in Fig. 6 shows rapid increases in both numbers and sizes with increasing distance from cloud base. In addition to the samples included in Fig. 6, the ice crystal concentration near cloud base was estimated as 8 l^{-1} of small hexagonal plate crystals (P1a) from a sample which could not be used to yield a complete size distribution.

The data in Fig. 6 suggest a production rate of 2 to 3 particles per liter per second of travel. The increasing widths of the size distributions reflect the growth of the crystals, together with continuous generation of new crystals and growth to detectable sizes. There may also be further factors contributing to the evolution of the size spectra, such as variability in the initial sizes of the ice particles, or variations in travel times arising from wind shear and turbulence.

c. 31 January 1975

One of the occasions when high concentrations of small ice crystals originating at the mountain surface extended to altitudes where they could be detected by the research aircraft is illustrated by this case.

The mountain on this day was enveloped by an altostratus layer which began about 30 km upwind (west) of Elk Mountain and extended some distance downwind of the mountain. Cloud top upwind of the mountain was at 4.3 km MSL and increased to 4.7 km over the mountain. This layer had a temperature range of −15° to −25°C and contained ice crystal concentrations (ICC) of 10 l^{-1} with little liquid water except near the mountain. The bottom diagram in Fig. 7 depicts this situation, showing the outlines of the ice cloud with a thin line and indicates the locations of two observed regions of liquid water by scalloped lines. The figure shows the track of the lowest altitude pass, and time traces for some of the measured parameters. The event of interest here is the sudden increase in ICC (based on data from the 2 D probe's shadow-or signal), by about a factor of 10, at 1132:40 MST, downwind of the mountain peak. The increase in ICC was accompanied by an increase in turbulence level.

Figure 8 provides further detail for this cloud pass from an analysis of crystal images from the 2D-C probe data. Each small horizontal line in the upper diagrams is derived from one record of 2D data (usually about 50 images, plus timing information). Artifact images (such as streaks or splashes of liquid water) were rejected in the computer processing of the data, but there were so few of these in this case that the ICC values were hardly affected. The top graph shows the ICC,

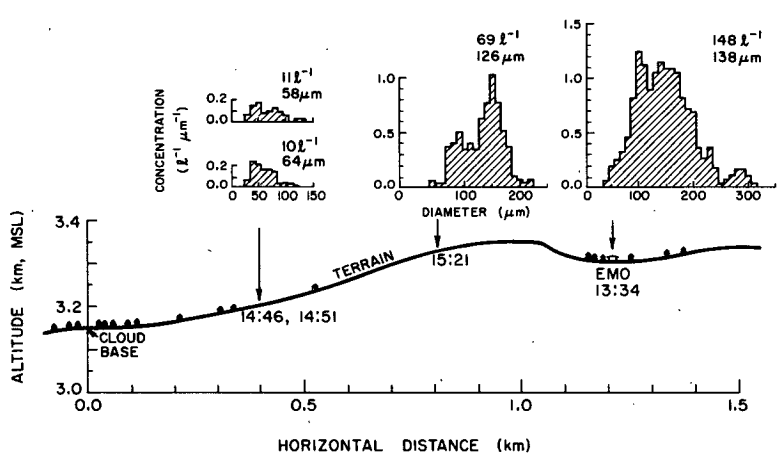

FIG. 6. Summary of ice crystal observations collected on 15 December 1978 at different sampling locations along the surface of the mountain. Wind flow in this diagram is from left to right. The evolution of the size spectra of ice crystals, with both the concentration and the mean size (values given in insets) increasing toward the EMO is clearly evident. Collection time (hr:min) is shown for each sample.

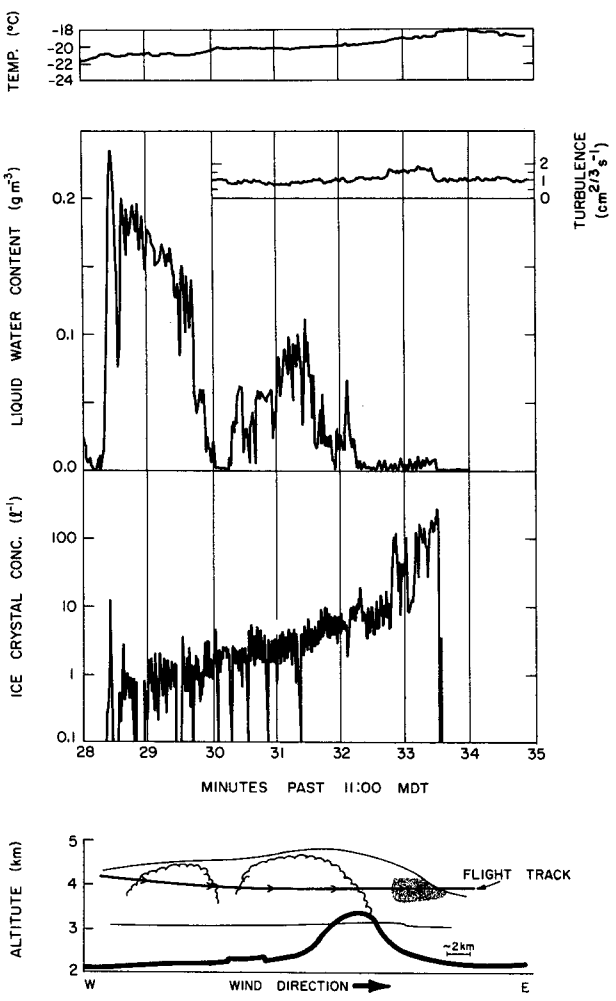

FIG. 7. Time trace of aircraft measurements along a cap cloud penetration in the downwind direction at 4.0 km MSL on 31 January 1975. The general outline of the cloud and the position of the flight track are shown in the sketch at the bottom of the figure. The scalloped lines in the sketch depict the regions of higher liquid water content. Ice crystal concentrations increased with distance into the cloud and showed a large increase at 1132:40 MST (also indicated by shading in the sketch). Changes in temperature and in the level of turbulence are seen at the same time.

and the bottom graph shows mean particle diameter for the size distribution of each record. The crystal sizes shown are the particle dimensions along the aircraft flight direction. Complete size distributions for three selected records are also shown; a correction for the dependence of sample volume on particle size is shown in dashed lines. The sample volume correction is also included in the top diagram of Fig. 8 which, therefore, indicates higher concentrations than those given in Fig. 7. The validity of these corrections (recommended by the instrument manufacturer) is not beyond question; the findings of Vali et al. (1981), for example, indicate that the uncorrected values are more likely to be right.

The main point in Figs. 7 and 8 is that they show the expected gradual increase in size and concentration throughout the cloud pass, and an unexpected sudden jump in concentration, due to smaller, uniform size crystals in the downwind portion of the cloud. The location of the zone of high ICC is shown by shading in the bottom diagram of Fig. 7. During aircraft passes at higher altitudes, the ICC was below 10 l^{-1} at all times. As shown in Fig. 7, even at the lowest altitude pass, the plume was intercepted just at the cloud boundary.

The location of the zone of high ICC was 600 m above and 4 km in the downwind direction from the summit and approximately 13 km downwind from where the cloud first contacted the mountain surface. It seems plausible that the zone of high ICC represents a "plume" of ice crystals from the surface. While the general airflow pattern over the mountain is a simple one, it is certainly complicated by small-scale disturbances in response to the complexities of the terrain. Mixing due to turbulence, flow separations at terrain slope discontinuities (e.g., Bradley, 1980; Fohn, 1980), or transient phenomena perhaps similar to snow devils may account for the transport of crystals from the surface to the point of observation. Blowing snow plumes even over flat surfaces have been observed to extend several hundreds of meters (Radok, 1977) and the ver-

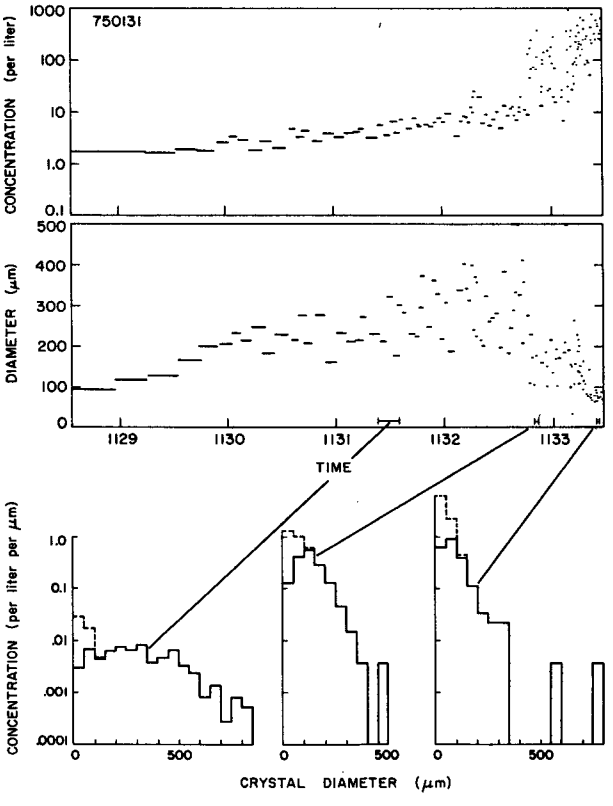

FIG. 8. Detail of the 2D-C probe data for the sequence shown in Fig. 7. Selected size distributions for three time periods are shown in histogram form at the bottom without and with sample volume correction (dashed).

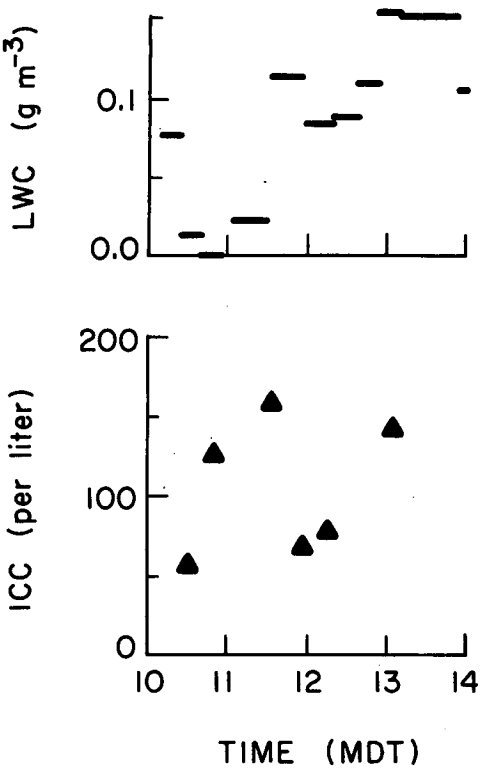

FIG. 9. Sequence of observations at the EMO on 31 January 1975 for the period bracketing the aircraft sampling shown in Figs. 7 and 8.

tical exchange coefficient for blowing snow can be ten times higher than what is expected from wind profiles (Businger, 1965). The small sizes of the crystals within the zone of high ICC indicate a relatively short lifetime consistent with a point of origin close to the summit. The observed increase in turbulence at the zone of high ICC also supports the notion of a localized turbulent plume; the stable atmospheric stratification and the lack of strong shear at the top of the cloud suggest that the most likely source of this turbulence is at the rough mountain surface.

The key observations at the EMO for the time period bracketing the aircraft sampling are shown in Fig. 9; temperature was −14°C and surface wind speed was around 25 m s^{-1}. The observed ICC were factors 5 to 10 higher than the values found by the aircraft through the main part of the cloud, and were comparable to the ICC in the downwind plume. Hence, these data suggest a surface origin for the small crystals.

d. 20 March 1975

This case illustrates high crystal concentrations in the downwind portion of an orographic cloud over a larger mountain range. The observations are from aircraft penetrations parallel to the wind in a shallow cloud layer over the Medicine Bow range, south of Elk Mountain. The Medicine Bow range is about five times wider than Elk Mountain and has approximately the same relief. The orographic cloud on 20 March 1975 had embedded convection and lasted throughout the day. The main cloud parameters are given in Table 1. Strong winds were present, and turbulence values doubled from the upwind side of the cloud to the downwind side. Figure 10 shows a portion of the ice crystal data collected along a flight path which passed approximately 1500 m above the terrain and 100 m below cloud top. These data exhibit the same features as those in Fig. 8: both the concentration and mean size of crystals gradually increase in the downwind direction (right to left in this diagram) until 1101 MST when a sudden increase in concentration and a decrease in mean size were observed. This change appears to be followed by fluctuations suggestive of weak convective elements, although this could not be confirmed by direct observations of up or downdrafts due to instrument limitations. A second aircraft pass an hour later and at a 200 m lower altitude showed a repetition of the same pattern. Surface observations were not available, but the data are sufficiently similar to the 31 January Elk Mountain case to suggest that the high concentrations resulted from the lifting of surface-generated crystals.

The extent of the region of high ice concentrations is significantly greater in this case than in the Elk Mountain case (nearly 10 km vs about 3 km), underscoring the possible importance of the phenomenon for the modification of cloud and precipitation characteristics.

e. 9 January 1975

This case study is presented as a counterexample, in which the ice concentrations observed at the EMO are

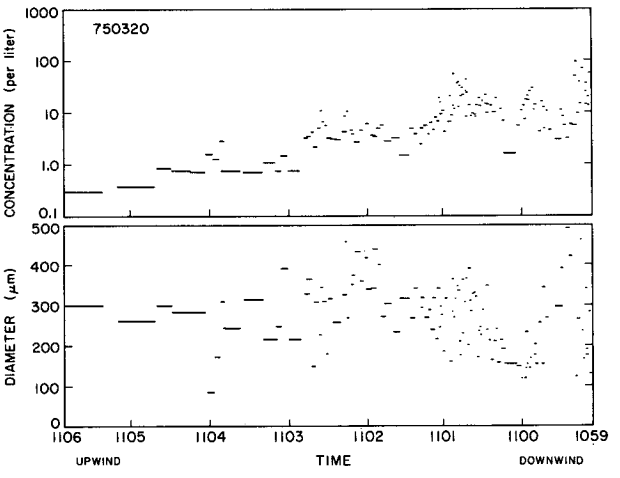

FIG. 10. Data collected with the 2D-C probe at 4.5 km MSL (−14.2°C) over the Medicine Bow Mountains on 20 March 1975. The presentation is the same as in Fig. 8, and the airflow in this case goes from left to right.

not anomalously high with respect to simultaneous aircraft measurements upwind.

An isolated cap cloud formed on this day in a post-frontal, stable air mass. Thin scattered cirrus were separated from the cap cloud by nearly 4 km of dry air (relative humidity < 50%). The cap cloud contained some small convective elements embedded in the otherwise steady airflow. Aircraft observations indicated that the convective elements became visually apparent at cloud top a short distance downwind of the leading edge and were advected through the cloud mass.

A summary of the data for this case is included in Table 1. Importantly, the concentrations of crystals measured aloft and at the surface were approximately equal; the differences in crystal habit and size are consequences of the differences in temperature and growth time. Wind speeds were lighter than during other cases discussed here.

At the EMO, the temperature changed less then 2°C and the winds remained nearly constant (±10%) in direction and speed during the 2 h of sampling. Crystal habits, sizes and concentrations varied appreciably only when convective elements passed over EMO. The convective elements added dendritic (P1f) crystals to the background of simple hexagonal plates (P1a). The dendritic crystals ranged in size from 1 to 3 mm diameter and were in concentrations of about 1 l^{-1} both aloft and at the surface.

The comparatively low values of ICC, and the fact that no differences were found between the observations aloft and at the surface suggest that in this case all ice crystals were formed by nucleation on aerosol with no generation of additional crystals at the mountain surface. It is not clear what differentiates this situation from the others; possibilities include lower wind speeds, different snow surface conditions, or other parameters not observed.

4. Ensemble data

The case studies described in the foregoing section demonstrate the major characteristics of the phenomenon we wish to analyze. In addition, a larger body of less-detailed data can be examined to reinforce and clarify the pattern suggested by the case studies. These aspects of the studies will be summarized in this section.

Our observations indicate that the high concentrations of small crystals develop only in the presence of a supercooled liquid cloud. The usual occurrence of cloud formation at EMO is that a cloud forms overhead, and then its base lowers with time, eventually enveloping the observatory. This corresponds to a period when humidity increases from below ice saturation to ice supersaturation and finally reaches slight water supersaturation. Crystal sampling throughout the time period during this lowering of cloud base usually shows that high ICC does not appear until the water cloud base is below EMO elevation and measurable LWC exists (>0.01 g m^{-3}).

Figure 11 shows the observed ICC versus temperature in isolated cap clouds from thirty sampling periods (on 26 days) for which simultaneous aircraft and EMO data were available. These data were condensed from detailed analyses for each day. Each aircraft datum is a geometric mean concentration over one cloud penetration.[1] The large open circles are for sampling upwind of the mountain summit, and the smaller filled circles are for sampling downwind. Each pass of approximately 5 km length represents about 250 L 2D-C probe sample volume. Typical spreads in temperature and ICC for each aircraft datum are ±0.5°C and a factor 2, respectively. Each EMO datum is a single measurement with the slide collection and photography technique. The EMO data cover the same time periods as the aircraft sampling.

The upwind concentrations of ice crystals correlate with temperature; r_{log}, the correlation coefficient between the temperature and the logarithm of ICC, is −0.63. From the monotonic rise in crystal concentrations with decreasing temperature (apart from the scatter) it appears nucleation near the clouds' leading edge is a reasonable explanation for the origin of these crystals. This view is supported by the initial rapid rise in ICC near cloud edge and relative uniformity of ICC through the cloud (Cooper and Vali, 1981), and by the rough agreement of crystal concentrations with ice nucleus concentrations (Vali et al., 1982).

The EMO data in Fig. 11, in accord with the earlier, independent data set from the EMO (Auer, 1971), show a similar trend with temperature as the aircraft data, although the numerical correlation between temperature and ICC is weaker than for the aircraft data. [Note that this pattern is different from the one reported by Hobbs (1969): he found concentrations at the Olympic Mountains, Washington to decrease with decreasing temperatures.] The main feature of interest here is that the concentrations observed at the EMO are roughly 100 times larger than the concentrations aloft. At any one temperature, a large range in ICC is apparent in the EMO data (geometric standard deviation is a factor of 4.8). Only about 5% of the data points overlap with the aircraft data, indicating that the situation shown for the 9 January 1975 case is quite rare. In the shallow cap clouds from which these data originate, there is no real possibility for ice to accumulate at some level or to move from colder regions to the points of observation. Therefore, the much higher ice crystal concentrations at the EMO are ascribable only to a phenomenon taking place in the air on its passage over the mountain surface toward the observatory.

[1] The geometric mean is used because the frequency distributions of concentration are close to lognormal in shape, and also, to reduce the sensitivity of the mean to extreme values. For a lognormal distribution with geometric standard deviation of 2 (typical of these data), the arithmetic mean is 1.27 times greater than the geometric mean.

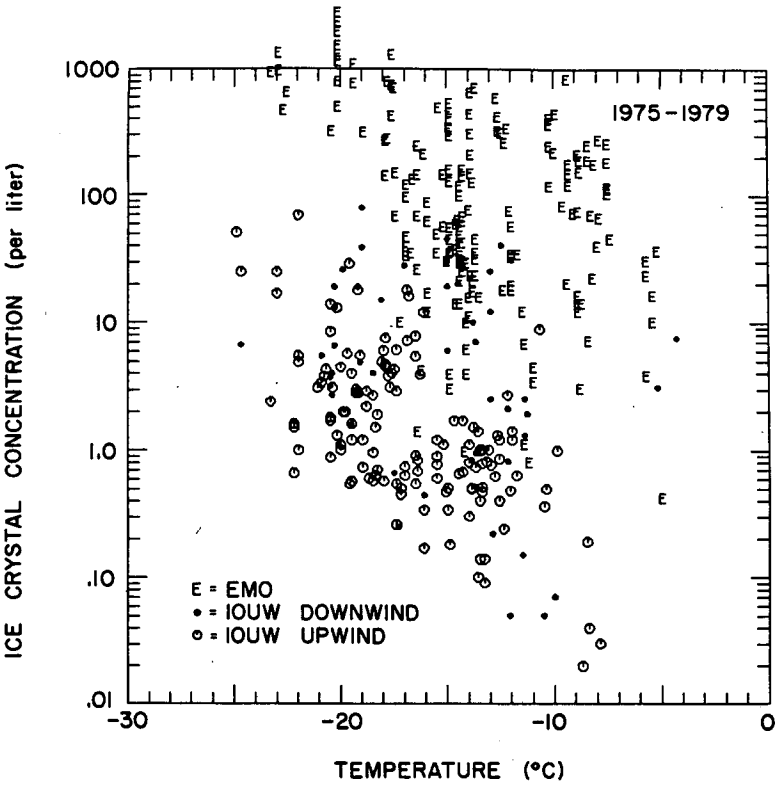

FIG. 11. A summary of ice crystal concentration measurements in Elk Mountain cap clouds. Each aircraft data point represents the geometric mean concentration and arithmetic mean temperature for one cloud pass (open circle) upwind or (closed circle) downwind of the mountain summit. Cloud passes were about 60 s in duration. Typical variabilities for these points are a factor of 2.0 in concentration (geometric standard deviation of the 1 s 2D-C probe counts during the pass) and ±0.5°C in temperature (standard deviation of 1 s values). Each EMO data point (E) is a separate measurement, taken coincidently with the aircraft observations. The data are from 30 different cloud cases on 26 days over the period 1975 to 1979.

The aircraft observations for the downwind portions of the clouds fall between the upwind and the EMO data. These points also cover a very large range in ICC (standard deviation is a factor 5.7), and the data are weakly correlated with temperature ($r_{\log} = -0.28$). The increase in concentrations for the downwind portions of the clouds with respect to the upwind concentrations is not negligible. Cooper and Vali (1981) showed evidence that no further nucleation usually takes place much beyond the cloud inflow region. Consequently, the downwind increases in Fig. 11 are likely due to the transport to flight levels of some of the high concentrations of crystals observed at the mountain surface.

The dependence of ice crystal concentrations at the EMO on wind speed is examined in Fig. 12. While there is no strong indication that, at any given temperature, the concentrations are governed by the wind speed, a slight trend toward higher concentrations with stronger winds may be discerned. Exceptions are also evident, but the whole database for this analysis is small, and parameters such as gust velocities may be better indicators than mean wind speeds.

A series of microphotographs of ice crystals collected at successively colder temperatures are given in Fig. 13, to amplify the comments made earlier with respect to the sizes and morphology of crystals observed at the EMO. The photographs in Fig. 13 were selected from different days and are representative of hundreds of samples collected during high ICC conditions. The samples have the following common features:

(a) The high concentrations of crystals are comprised of relatively uniform populations of small (<100 μm) crystals.

(b) The growth habits of the small crystals follow the expected pattern of dependence on temperature.

(c) There are always large numbers of blowing snow and dislodged rime particles on the slides, along with the pristine, vapor-grown crystals. Our impression is that there is no relationship between the numbers, characteristics and sizes of the irregular ice particles and the vapor-grown crystals, but this aspect of the observations has not yet been systematically pursued.

(d) Within the temperature range of plate growth

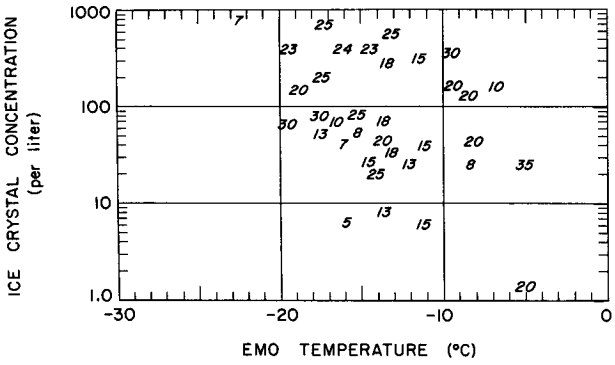

FIG. 12. Average ice crystal concentrations and temperatures for 35 clouds (on 30 days, in the period 1974 to 1979), with the wind speed observed at 10 m above the surface indicated for each point. A trend is apparent for higher concentrations to accompany higher wind speeds.

(−10° to −20°C), the majority of crystals are double structured. This structure is usually interpreted as the result of diffusion growth onto the most widely separated a-axes of monocrystalline ice particles which had considerable size (10 μm or more) before crystal growth began (Auer, 1971; Jiusto and Weickmann, 1973). As discussed in the 15 December 1978 case study, the interpretation of the origins of these crystal centers is ambiguous.

(e) Riming is observed on the very few crystals larger than ~200 μm, but in Elk Mountain cap clouds such riming is minor because of the short time available and because of the low liquid water contents. The pattern and extent of riming on the crystals is similar to what has been observed elsewhere.

5. Growth histories

Calculations were made of the growth and evaporation of ice particles along the trajectories upwind of and in the cap clouds, along the mountain surface, in order to gain some insight into the possible locations of the origins of the "anomalous" crystals observed at the EMO. Appendix A gives the details of the model and the initial values assumed.

An example of the results of the calculations is shown in Fig. 14 for ten different initial sizes of crystals starting 500 m below cloud base and rising in a 2 m s^{-1} updraft. The traces, moving upwards, show the initial evaporation and subsequent growth of the particles. By interpolation between lines, the growth histories of crystals of other initial sizes can also be followed. The same calculations show that a 1 μm particle starting at the point where ice saturation is reached would be 100 μm in size 250 m above cloud base. Ice particles below the heavy solid line in Fig. 14 evaporate completely before reaching the ice saturation zone.

The dependence of growth on updraft velocity is shown in Fig. 15 for initially 100 μm particles. These results reveal that the updraft has to exceed ~2.5 m s^{-1} for particles of this size to survive transit through the 350 m deep evaporation region. Beyond that threshold value, the magnitude of the updraft plays only a minor role in determining crystal size.

The observed crystal sizes at three different locations from the 15 December case study are plotted with the model predictions in Fig. 15. The updraft speed was estimated from the observed wind to be 3 m s^{-1}. The comparison indicates that the observed sizes could not have been reached by growth from submicron nuclei or ice particles within the time available. For example,

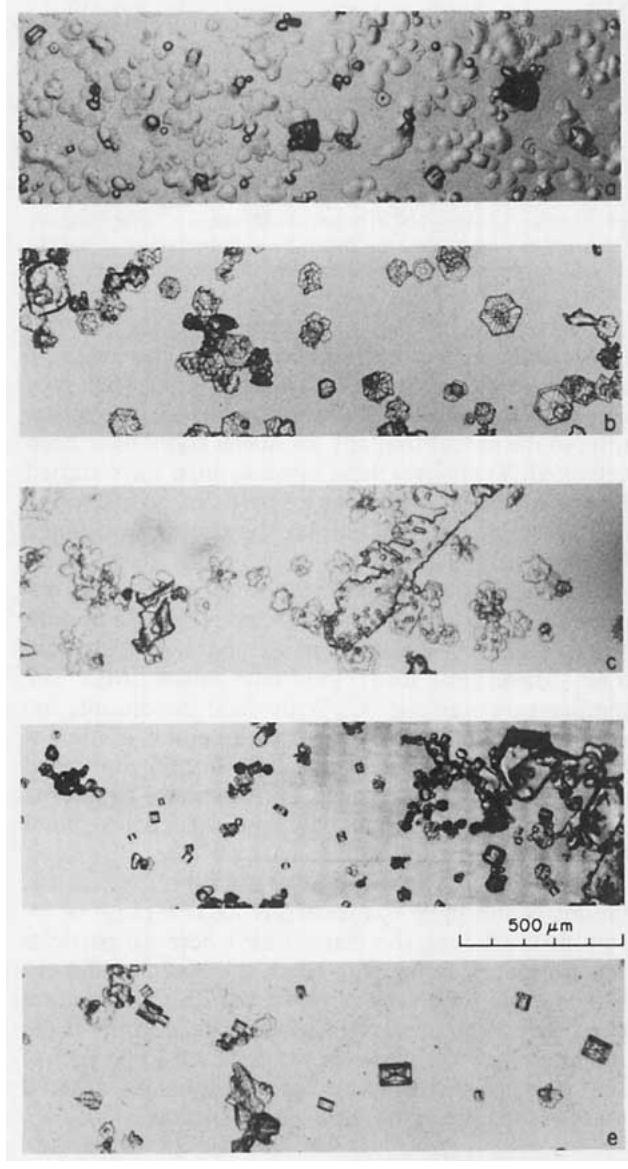

FIG. 13. Ice crystal samples from EMO during high ICC conditions. Date, temperature and ICC for the samples are: (a) 18 January 1979, −7.3°C, 110 l^{-1}; (b) 24 March 1976, −10.0°C, 620 l^{-1}; (c) 16 January 1979, −12.4°C, 595 l^{-1}; (d) 7 January 1976, −20.2°C, 1940 l^{-1}; and (e) 10 January 1975, −23.0°C, 1320 l^{-1}. Width of photographs correspond to 1.9 mm.

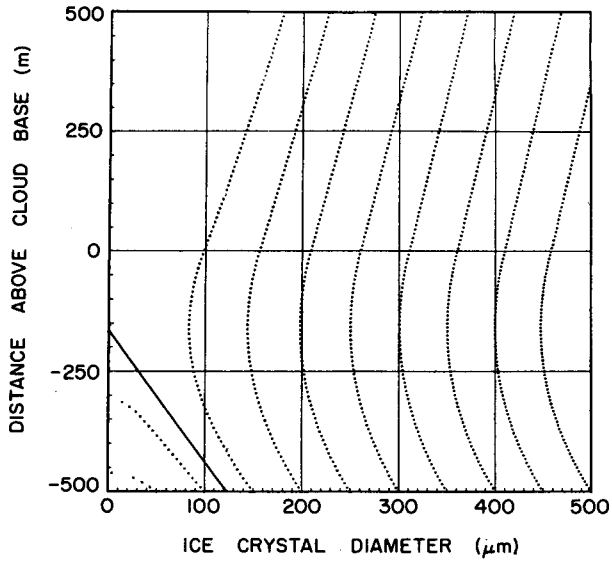

FIG. 14. Model predictions of the evaporation or growth of single ice crystals originating 500 m below cloud base in a 2 m s^{-1} updraft. Crystal sizes evolve along the dotted lines, from bottom to top. To the left of the tilted full line the crystals evaporate completely.

the crystals observed 80 m above cloud base with 58 μm mean size must have been 20 to 30 μm when they ascended through ice saturation, which is the earliest time in the ascent that any ice nuclei could have been activated. Therefore, these crystals must have started growth from relatively large ice particles, or had to follow trajectories more complex than those envisioned for the calculations.

It is easier to account for the small crystal sizes observed in the 18 February 1975 case (Figs. 3a and 4). Winds for this case give a 5 m s^{-1} updraft velocity and a 60 s travel time from cloud base to the EMO. The temperature was −18°C. With these conditions, the sizes corresponding to the half-width points of the distribution in Fig. 4 can be attained from 1 μm initial sizes in 41 and 98 s of growth, corresponding to starting points 100 m above cloud base and 200 m below cloud base (near ice saturation), respectively.

The deduction that can be made from these calculations is that there is a relatively narrow range of locations bracketing the cloud base where ice particles must originate in order to reach the observed dimensions by the time they arrive at the EMO. There are cases where the observations are matched only if the initial sizes of the particles are assumed to be tens of μm, or if longer growth times are somehow allowed than what is predicted for a simple airflow.

6. Possible mechanisms

The observations and calculations summarized in the foregoing sections allow some definition of the possibilities which need to be considered in accounting for the "anomalous" crystal production at the mountain surface. To aid this step, the main features of the phenomenon are briefly restated:

(a) The main ingredients for the process to become active are the presence of a supercooled cloud and a snow- or rime-covered mountain surface. The clouds typically consist of droplets of <10 μm diameter and water contents of <0.2 g m^{-3} (Politovich and Vali, 1983). We have no specific observations of characteristics of the snow surface or of the rime that could be correlated with the crystal production.

(b) The process was found to be active at temperatures ranging from −5°C to −25°C. At all temperatures within this range, the increases over the free-cloud concentrations of ice crystals are approximately 100-fold. No observations are available for temperatures outside the indicated range, so the actual limits are not known.

(c) The process yields crystals of the same appearance as other origins. Crystal habits are determined by the temperature, and crystal embryos are either submicroscopic in size, or are less than a few tens of μm originally and are merged into the crystal structure without noticeable discontinuity (except in the case of double crystals where the embryos are distinguishable but not really identifiable).

(d) The sizes of the crystals can be accounted for by vapor growth if the crystals are assumed to originate along the traverse of the air over the mountain slope starting perhaps as soon as ice saturation is reached.

There are a number of possible processes of gener-

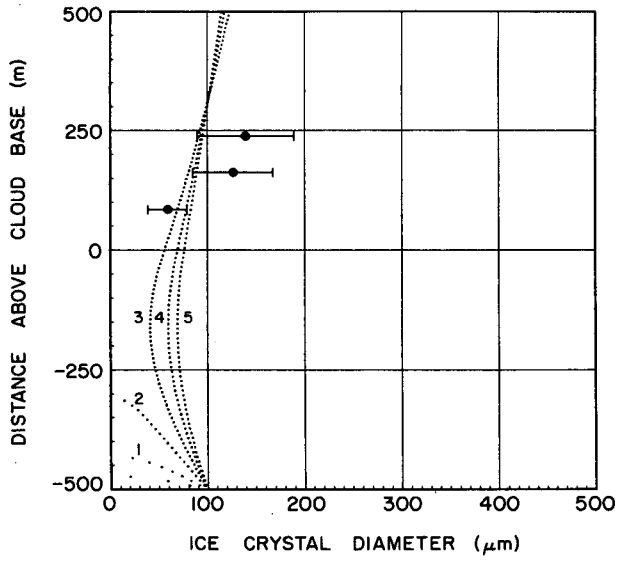

FIG. 15. Similar to Fig. 14, but for a single 100 μm crystal starting 500 m below cloud base and ascending in an updraft of 0.5, 1, 2, 3, 4 or 5 m s^{-1}. Large dots and horizontal bars show observed mean sizes and standard deviations, respectively, from the 15 December 1978 case study (Fig. 6).

ation of the anomalous crystal concentrations which should be examined. The list is not much different from the one which was considered in search of the processes of ice multiplication in clouds (Mossop, 1970), but there are both simplifying and complicating factors to include.

Since the air feeding the clouds is from a relatively uniform source, and the ground is snow covered even in the upwind valley, there is no basis for arguing the presence of local sources of ice nuclei which could affect the lowest layer of the air ascending the mountain. The crystal concentrations are also of much higher magnitude than any ice nucleus measurements have ever yielded. The possibility of preactivation of nuclei in the air just above the snow surface is more real. It is conceivable that exposure of nuclei to the moisture field of evaporating ice (below cloud base) will condition some aerosol particles to become ice nuclei. Also, residues of evaporating snow particles might act as preactivated nuclei; Roberts and Hallett (1968) showed evidence for such a process to work. Neither of the possible preactivation processes can be tested against the available data; experimental tests are possible with appropriate simulation of the conditions of the snow surface. Such tests could be of even greater interest than the specific problem discussed in this paper as there may be a wide contribution to atmospheric ice nuclei by such processes.

The ice multiplication, or secondary generation, processes shown to be effective in some clouds can be ruled out for the mountain effect discussed here. The Hallett-Mossop (1974) mechanism of ice splintering is effective only over a limited temperature range and requires the presence of cloud droplets at sizes which do not exist in the cap clouds. The possibility that riming is related in some way to the generation of the high crystal concentrations cannot be ruled out; in fact, the extensive riming on trees, rocks and the snow surface provides very large numbers of riming events, orders of magnitude more than is occurring through riming on ice crystals in clouds. If there is even a low probability for splinter production by riming events under the prevailing conditions, such a process might explain the observations. Splinter production probabilities much lower than could be detected in past experiments would appear to be sufficient, although we are not able to give quantitative estimates at this time.

Crystal fragmentation (Hobbs and Farber, 1972; Vardiman, 1978) seems to be ruled out by the absence of ice crystals of millimeter sizes. Similarly, the fragmentation of drops freezing in free fall can be discounted because of the low efficiency of this process even at droplet sizes of >40 μm (Bader et al., 1974), and because there is no evidence at all for fragmentation to be occurring with the small droplet sizes present in the cap clouds. The mechanism proposed by Hobbs and Rangno (1985) would require the presence of cloud droplets of >20 μm diameter, which are extremely rare in Elk Mountain cap clouds (Politovich and Vali, 1983).

A further possibility which needs to be examined is that the high concentrations of ice crystals arise from the lifting of snow particles from the surface, i.e., blowing snow. The general characteristics of blowing snow are summarized in the reviews of Mellor (1965), Radok (1977) and Schmidt (1982). Above a threshold value of wind speed, snow particles are lifted from the surface and travel by creep, saltation and advection to considerable distances before becoming redeposited. Both particle size and concentration decrease with altitude and increase with wind speed. Particle concentrations as high as $1000\,l^{-1}$ at 1 m elevation are common. Large variabilities in the characteristics of blowing snow arise from variations in the nature and history of the snow surface, and from differences in meteorological parameters such as temperature, humidity, wind speed and gustiness.

To simulate the size distributions which may result from blowing snow at the EMO, calculations similar to those in section 5 were performed. The details of the model are described in appendix B. Results are shown in Figs. B2, B3 and B4 for the situation where the injection of snow particles into the air stream is assumed to be taking place at all points along its travel. There is a reasonable match to the observations of the 15 December 1978 case, as shown by the horizontal bars in Fig. B3 and by a comparison of Fig. B4 with Fig. 6. These calculations of crystal sizes support the plausibility of explaining the observed high ice concentrations as blowing snow. The difficulty with the explanation is that blowing snow particles are expected to have irregular shapes, at least when they leave the snow surface, yet the growth calculations and the matching observations are for vapor-grown crystals of symmetrical habits. This discrepancy can be bridged to some extent by the suggestion that the snow surface in contact with a supercooled cloud will have crystals grown from the vapor by the Bergeron process. However, we know of no evidence for crystals of the order of 100 μm to be found on snow surfaces and consider it unlikely that they in fact exist. Hoarfrost is known to form in ice supersaturated air without the presence of supercooled cloud droplets. The crystal shapes of hoar are distinctly different from those found in clouds. In the presence of a supercooled cloud the snow surface will undoubtedly be growing by deposition and by riming, but little is known of the details of the characteristics that may develop. Another possibility is that some blowing snow particles are small enough to be transformed into the observed shapes by the growth taking place during their airborne travel. This assumption is not supported by the available data regarding the sizes of snow particles lifted into the air (see Fig. B1), but the presence of particles <10 μm is difficult to detect and previous tests have not well represented the conditions of concern here (especially the simul-

taneous presence of a cloud over the snow surface). Thus, the importance of blowing snow in the generation of the observed ice crystals cannot be fully evaluated without further tests.

7. Conclusions

The presence of large concentrations of small ice crystals was frequently observed within supercooled clouds passing over snow surfaces. The range of conditions for these events to occur is already known to be very broad and may be even broader than what has been covered by our set of observations. The evidence is consistent with the suggestion that the "anomalous" crystals are generated near the snow surface and that they are subsequently carried to substantial heights (up to 1 km in the available observations) within the clouds.

The mechanism responsible for the generation of the crystals is not yet known. The main possibilities appear to be related either to the riming taking place on the snow and other surfaces, or to the lifting of pre-existing particles from the snow surface. Future investigations of the phenomenon may uncover interesting links with the secondary ice generation taking place in clouds.

The frequent occurrence of the phenomenon and the magnitude of the increases in crystal concentrations compared to undisturbed conditions, suggest that there may be significant implications for the evolution of supercooled clouds over mountain ranges. The lifetimes, radiative properties, propensities to form precipitation, etc., of the clouds may thus be influenced. There is also an important consequence for the prospects of modifying such clouds by the addition of artificial ice nuclei. The importance of wintertime orographic clouds to annual precipitation amounts in the western United States, and in many other parts of the world, underscores the significance of understanding the production of ice crystals at mountain surfaces. This type of cloud microphysical influence of mountains has not been considered in the past and adds a further dimension to the studies of orographic clouds.

Acknowledgments. This research was sponsored by the Meteorology program, Atmospheric Science Section, National Science Foundation Grant ATM77-17540. The financial support of the NSF, and the support of the pilots, engineers, technicians and other staff of the Department of Atmospheric Science, University of Wyoming, are gratefully acknowledged. Model development and computations were done at the University of Wyoming, the Alberta Research Council and Colorado State University. Constructive comments by the reviewers led to several clarifications in the text.

APPENDIX A

Single Particle Growth Model

The model is designed to study the diffusion growth or evaporation of falling ice particles in a steady updraft. The basic model has two components: one part calculates snow particle growth, evaporation and sedimentation, and the other part calculates the thermodynamic state parameters in an adiabatically ascending air parcel which contains the crystal. The equation for snow particle growth and evaporation follows the usual treatment of diffusion growth (e.g., Pruppacher and Klett, 1978). The mass growth rate is:

$$\frac{dM}{dt}=\frac{4\pi C(S_i-1)}{A+B}f_v f_w \tag{A1}$$

where

$$A=\frac{L_s}{kT}\left(\frac{L_s}{kT}-1\right) \tag{A2}$$

$$B=\frac{R_v T}{\delta e_i(T) f_{3b}}. \tag{A3}$$

Variables are defined in Appendix C. Numerical values for the thermodynamic quantities were taken from the Smithsonian Meteorological Tables (List, 1949). The additional factor f_w in (A1) is used to account for the enhancement in growth rate in the presence of a liquid water cloud (Marshall and Langleben, 1954)

$$f_w=1+\frac{1}{2}D\left(\frac{4\pi}{N_d}\right)^{1/3}(3\chi)^{1/6} \tag{A4}$$

and the factor f_v in (A1) accounts for ventilation (Jayaweera, 1971).

$$f_v=1+\frac{0.6\mathbb{P}}{4\pi C}\sqrt{\mathrm{Re}^*} \tag{A5}$$

The factor f_{3b} accounts for ice-surface kinetic effects through the deposition coefficient (Fukuta and Walter, 1970):

$$f_{3b}=\frac{1}{1+(2\delta/D\beta)(2\pi/R_v T)^{1/2}}. \tag{A6}$$

Saturation vapor pressures are calculated using the Goff-Gratch equations (Goff, 1949). The mass growth rate in (A1) was transformed into diameter growth rate using the mass-diameter relationships for different crystal types given by Davis (1974). The resulting equation was integrated with a fourth-order Runge-Kutta method.

Crystal habits in the model were chosen to be appropriate to the particle size and the ambient temperature and humidity. For this study, we chose temperatures in the range $-10°$ to $-13°$C, where Magono and Lee (1966) indicate that thick plate crystals (C1g) grow below water saturation, and simple hexagonal plate crystals (P1a) grow at and slightly above water saturation. In the model, crystals fall at their terminal velocity relative to the updraft: particles < 20 μm diameter are considered to be ice spheres which follow Stokes' fall velocity; larger particles are either thick plate

or hexagonal plate crystals and fall according to equations given by Davis (1974). The rate of change of the crystal altitude is:

$$\frac{dZ}{dt} = W - V_t. \quad \text{(A7)}$$

In the second component of the model, the thermodynamic properties of the environment are calculated at the location of the particle after each time step. The hypsometric equation is used to calculate the parcel pressure change corresponding to the altitude change given by (A7). Below cloud base, the parcel ascent (or descent) is dry adiabatic; temperature is calculated from Poisson's equation, and dewpoint is found in an iterative procedure that conserves mixing ratio. Above cloud base, the ascent is saturation pseudoadiabatic; temperature and dewpoint are calculated by an iterative procedure that conserves equivalent potential temperature.

Above cloud base, the concentration of cloud droplets is arbitrarily held constant at 300 cm^{-3}, a typical value for Elk Mountain clouds (Politovich and Vali, 1983). In the model, the water mass balance is a constraint only for water vapor and liquid water; to simplify the model, ice mass was not included. Thus, as the parcel ascends above cloud base, liquid water condenses to keep the environment at water saturation, even when an ice crystal is present. This is probably not realistic for high concentrations of ice crystals. In blowing snow situations, the mass of airborne ice varies strongly in the vertical. For example, Budd et al. (1966) measured snow drift densities of 1000 g m^{-3} at 0.01 m height and 1 g m^{-3} at 1.0 m for 15 m s^{-1} wind speeds (at 10 m). The effect of large drift density is to force the vapor density to be close to ice saturation (e.g., 1.8 g m^{-3} at −12°C). The model is clearly in error within 1 m of the surface; there, it will overpredict growth and evaporation rates. At heights above about 10 m, it becomes more reasonable.

Initial values are specified for temperature, dewpoint, pressure, updraft speed and ice crystal size. For calculations representing the 15 December 1978 case study, model initial values were chosen to be 500 m below cloud base: pressure 750 mb, temperature −7.1°C, and dewpoint −11.2°C. The cloud base is at 700 mb and −12°C, typical values for Elk Mountain cap clouds (Rogers and Politovich, 1981). Model updraft speeds were in the range 0.5 to 5 m s^{-1}, and were inferred from the observed range of wind speeds at Elk Mountain, multiplied by the sine of the terrain slope. Time steps were usually chosen to give 10 m vertical displacements of the parcel. The output of the model is a prediction of the snow crystal size and location as a function of time. The computation stops when particle size lies outside of the range 1.0 μm–500 μm or when the particle has been lifted 500 m above cloud base.

APPENDIX B

Multiple Particle Growth Model

In another version of the model which is described in appendix A, many ice particles are added to the air parcel, and the evolution of the size distribution is calculated. The size distribution of blowing snow added to the air parcel is described by a two-parameter Gamma function with values representative of 2 m above the surface: mean size 100 μm and standard deviation 50 μm, as shown in Fig. B1. Three ideas were explored for adding particles: (A) at the first time step only (This is the case where there is a single source region.); (B) at every time step (This describes the case where blowing snow is produced during the entire ascent.); and (C) at every time step below ice saturation, with none added above. Simulation C tries to account for the effect of humidity on blowing snow production—less production is expected above ice saturation because vapor growth increases the mass of surface snow particles, the adhesion between particles is stronger (Hosler et al., 1957), and particles are sintered together (Hobbs and Mason, 1964).

At each time step, the snow particles are sorted into 1 μm wide size bins. Particles fall with respect to the updraft at the speed of the average size particle. Snow crystals are removed by two processes: all those larger than 500 μm are considered too large to remain airborne as blowing snow, and those smaller than 1 μm are considered to have evaporated completely. At any one time, the size distribution typically consists of several hundred to several thousand particles.

The model results from simulation A with updrafts of 0.5, 1, 2 or 4 m s^{-1} are shown in Fig. B2. The lines trace the histories of the average size. In the 0.5 m s^{-1} updraft, the entire size distribution evaporates, even though the largest initial particle was 212 μm. In the

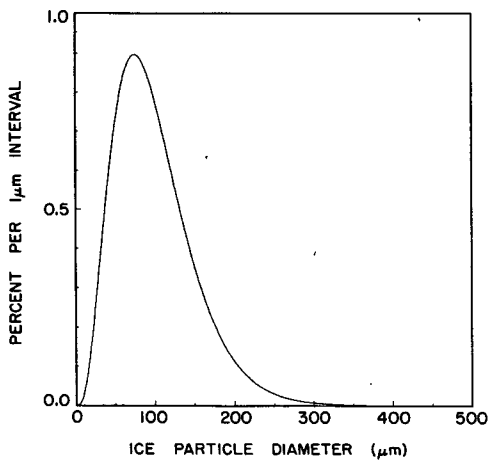

FIG. B1. Normalized size distribution of blowing snow, as defined by a two-parameter Gamma function with mean of 100 μm and standard deviation of 50 μm (after Schmidt, 1981).

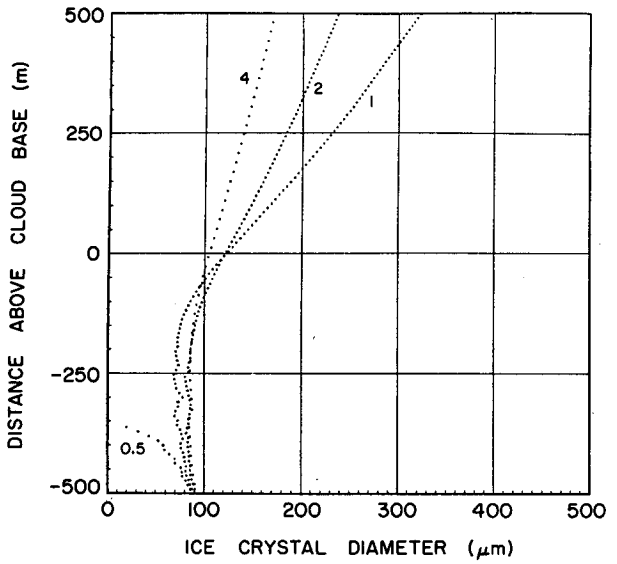

FIG. B2. Model predictions of evaporation or growth of an ensemble of ice particles, ascending in updrafts of 0.5, 1, 2, or 4 m s^{-1}. Blowing snow particles (Fig. B1) were introduced only at the first time step, 500 m below cloud base. The dotted lines show the evolution of the mean diameter, from the bottom toward the top of the figure.

faster updrafts, some of the larger particles reach the ice supersaturated region. Of the initial 1039 particles, the fractions which ultimately reach cloud base are 9%, 46% and 74% for updrafts of 1, 2 and 4 m s^{-1}, respectively. Wiggles in the lines are an artifact of the analysis because of the small remaining sample size.

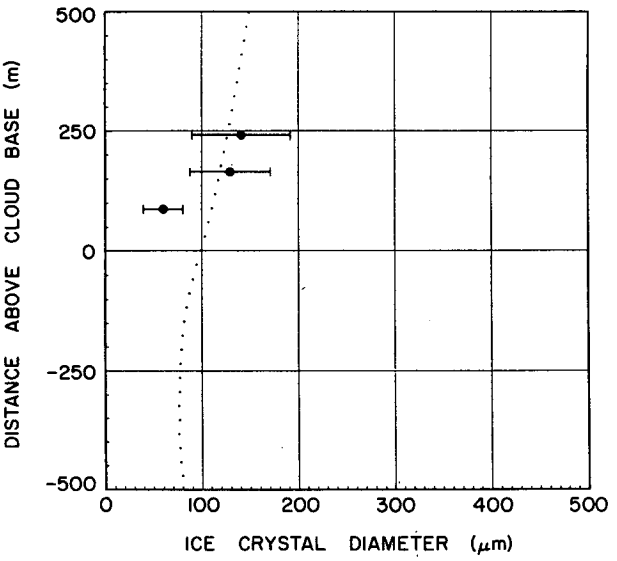

FIG. B3. Similar to Fig. B2, with constant updraft 3 m s^{-1} and with blowing snow particles added to the ensemble at each time step of 10 s. Large dots and horizontal bars show the observed mean sizes and standard deviations from the 15 December 1978 case study (Fig. 6).

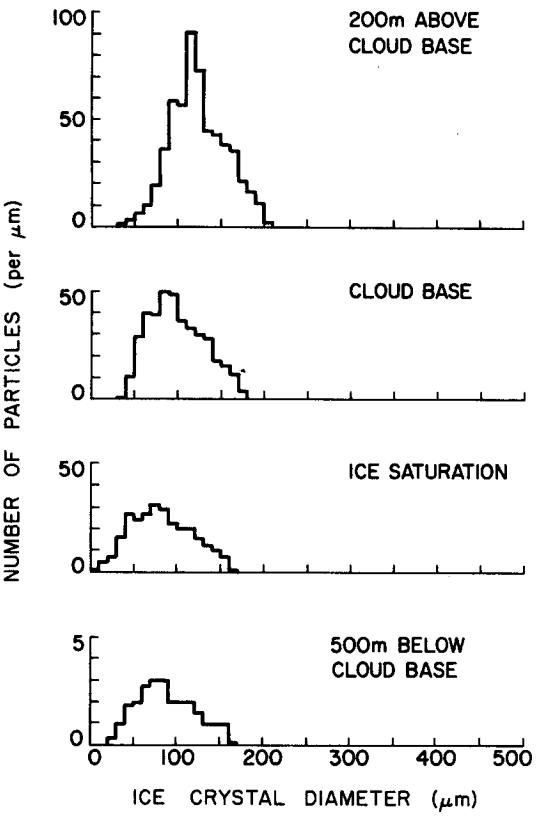

FIG. B4. Ice particle size distributions from the model simulation in Fig. B3 at four particular locations. Ordinate scale for the bottom plot is exaggerated tenfold compared to others.

The model results from simulation C are shown in Fig. B3. The updraft in this simulation is 3 m s^{-1} and corresponds with the 15 December 1978 case study. The addition of 245 particles at every time step (10 s) moderates the evolution of the size distribution, so that the mean size changes slowly. Of the 2940 particles added below ice saturation, 2463 (84%) reach cloud base. The standard deviation of the size distribution changes slightly over the total 1000 m ascent, from a minimum of 30 μm to a maximum of 40 μm.

Examples of size distributions from this simulation are shown in Fig. B4 for four particular locations: 500 m below cloud base; at ice saturation; at cloud base; and 200 m above cloud base. The data were grouped into 10 μm intervals for plotting; computational resolution in the model is 1 μm. Notice that each of these distributions is relatively narrow and has one prominent mode. These distributions can be compared with those from the case study in Fig. 6. The shapes and evolution of the observed and model size distributions are remarkably similar.

Model simulations using version B are not shown. They are similar to C, but the distributions are slightly narrower above ice saturation.

The significance of the model results is that there is a realistic range of particle sizes and atmospheric conditions for which blowing snow particles can survive transport through an evaporation region and enter a supercooled orographic cloud. The predicted size distributions are in general agreement with the observations. Strong winds lead to a greater likelihood of this happening because transit time through ice subsaturation is reduced, more blowing snow is produced (given the same snow cover), larger particles are produced and turbulent mixing within the surface layer is enhanced.

APPENDIX C

Definitions of Terms Used in Equations

C	capacitance
D	diameter of circle enclosing plate family crystal
e_i	saturation vapor pressure over ice
f_{3b}	surface kinetics factor
f_v	growth enhancement factor from ventilation
f_w	growth enhancement factor from water cloud
k	thermal conductivity of air
L_s	latent heat of sublimation
M	mass of crystal
N_d	number concentration of cloud droplets
$\mathbb{P}$	perimeter of crystal in the plane normal to direction of fall
Re*	Reynolds number of crystal characteristic dimension falling at terminal velocity in air
R_v	ideal gas constant for water vapor
S_i	supersaturation of water vapor relative to ice at the same temperature
t	time
T	temperature of air parcel
W	updraft
Z	altitude of crystal
β	deposition coefficient for water molecules onto ice (0.04)
δ	diffusivity of water vapor in air
χ	liquid water content

REFERENCES

Auer, A. H., Jr., 1971: Observations of ice crystal nucleation by droplet freezing in natural clouds. *J. Atmos. Sci.*, **28,** 285–290.

Bader, M., J. Gloster, J. L. Brownscombe and P. Goldsmith, 1974: The production of submicron ice fragments by water droplets freezing in free fall or on accretion upon an ice surface. *Quart. J. Roy. Meteor. Soc.*, **100,** 420–426.

Blyth, A. M., T. W. Choularton, G. Fullarton, J. Latham, C. S. Hill, M. H. Smith and I. M. Stromberg, 1980: The influence of entrainment on the evolution cloud droplet spectra. II: Field experiment at the Great Dun Fell. *Quart. J. Roy. Meteor. Soc.*, **106,** 821–840.

Borys, R. D., P. J. DeMott, E. E. Hindman and D. Feng, 1983: The significance of snow crystal and mountain surface riming to the removal of atmospheric trace constituents from cold clouds. In: *Precipitation Scavenging, Dry Deposition and Resuspension,* Vol. 1. H. R. Pruppacher, R. G. Semonin and W. G. N. Slinn (coord.), Elsevier Press, 181–190.

Bradley, E. F., 1980: An experimental study of the profiles of wind speed, shearing stress and turbulence at the crest of a large hill. *Quart. J. Roy. Meteor. Soc.*, **106,** 101–123.

Budd, W. F., W. J. R. Dingle and U. Radok, 1966: The Byrd snow drift project: Outline and basic results. In: *Studies in Antarctic Meteorology,* M. J. Rubin, Ed., Vol. 9., Amer. Geophys. Union, 71–134.

Businger, J. A., 1965: Eddy diffusion and settling speed in blown snow. *J. Geophys. Res.*, **70,** 3307–3313.

Cooper, W. A., and C. P. R. Saunders, 1980: Winter storms over the San Juan Mountains. Part II: Microphysical processes. *J. Appl. Meteor.*, **19,** 927–941.

——, and G. Vali, 1981: The origin of ice in mountain clouds. *J. Atmos. Sci.*, **38,** 1244–1259.

Davis, C. I., 1974: The ice nucleating charcteristics of various AgI aerosols. Ph.D. Dissertation, University of Wyoming, Laramie, 267 pp.

Diem, M., 1962: Zur Struktur der Wolken. *Arch. Met. Geoph. Biokl. A.*, **13,** 34–56.

Fohn, P. M. B., 1980: Snow transport over mountain crests. *J. Glaciol.*, **26,** 469–480.

Fukuta, N., and L. A. Walter, 1970: Kinetics of hydrometeor growth from a vapor-spherical model. *J. Atmos. Sci.*, **27,** 1160–1172.

Goff, J. A., 1949: Final report of the working subcommittee of the international joint committee on psychrometric data. *Trans. Amer. Soc. Mech. Engr.*, **71,** 903–913.

Hallett, J., and S. C. Mossop, 1974: Production of secondary ice particles during the riming process. *Nature,* **249,** 26–28.

Hobbs, P. V., 1969: Ice multiplication in clouds. *J. Atmos. Sci.*, **26,** 315–318.

——, and R. J. Farber, 1972: Fragmentation of ice particles in clouds. *J. Rech. Atm.*, **6,** 245–258.

——, and B. J. Mason, 1964: The sintering and adhesion of ice. *Phil. Mag.*, **9,** 181–197.

——, and A. L. Rangno, 1985: Ice particle concentrations in clouds. *J. Atmos. Sci.*, **42,** 2523–2549.

Hosler, C. L., D. C. Jensen and L. Goldshlak, 1957: On the aggregation of ice crystals to form snow. *J. Meteor.*, **14,** 415–420.

Jayaweera, K. O. L. F., 1971: Calculations of ice crystal growth. *J. Atmos. Sci.*, **28,** 728–736.

Jiusto, J. E., and H. K. Weickmann 1973: Types of snowfall. *Bull. Amer. Meteor. Soc.*, **54,** 1148–1162.

Kohler, H., 1925: Untersuchungen uber die Elemente des Nebels und der Wolken. *Medd. meteor.-hydr. Anst. Stockh.*, **2,** No. 5.

Kuettner, J., 1950: The electrical and meteorological conditions inside thunderclouds. *J. Meteor.*, **7,** 322–332.

Langmuir, I., 1948: Summary of results thus far obtained in artificial nucleation of clouds. Res. Lab. Rept. RL-140., General Electric Co., reprinted in the Collected Works of Irving Langmuir., Vol. 11. Pergamon Press, pp. 3–18.

List, R. J., 1949: *Smithsonian Meteorological Tables,* Smithsonian Inst. Press, 527 pp.

Magono, C., and C. W. Lee, 1966: Meteorological classification of natural snow crystals. *J. Fac. Sci., Hokkaido Univ.,* Series VII, **2,** 321–362.

Marshall, J. S., and M. P. Langleben, 1954: A theory of snow-crystal habit and growth. *J. Meteor.*, **11,** 104–120.

Mellor, M., 1965: Blowing snow. *Cold Regions Science and Engineering.* Part III, Section A3c. Cold Regions Res. and Eng. Lab., Hanover, 85 pp.

Mossop, S. C., 1980: Concentrations of ice crystals in clouds. *Bull. Amer. Meteor. Soc.*, **61,** 474–479.

Politovich, M. K., and G. Vali, 1983: Observations of liquid water in orographic clouds over Elk Mountain. *J. Atmos. Sci.*, **40,** 1300–1312.

Pruppacher, H. R., and J. D. Klett, 1978: *Microphysics of Clouds and Precipitation,* D. Reidel Publ. Co., 714 pp.

Radok, U., 1977: Snow drift. *J. Glaciology,* **19,** 123–139.

Ranz, W. E., and J. B. Wong, 1952: Impaction of dust and smoke

particles on surface and body collectors. *Ind. Eng. Chem.*, **44,** 1372–1381.

Rittberger, W., 1959: Zur Struktur der Wolken. *Arch. Met. Geoph. Biokl. A.*, **11,** 333–367.

Roberts, P., and J. Hallett, 1968: A laboratory study of the ice nucleating properties of some mineral particulates. *Quart. J. Roy. Meteor. Soc.*, **94,** 25–34.

Rogers, D. C., and M. K. Politovich, 1981: Meteorology of the wintertime Elk Mountain cap cloud. *Second Conf. on Mountain Meteorology,* Steamboat Springs, Amer. Meteor. Soc., 371–374.

——, D. Baumgardner and Gabor Vali, 1983: Determination of supercooled liquid water content by measuring rime rate. *J. Appl. Meteor.*, **22,** 153–162.

Saunders, C. P. R., 1978: Electrification experiments on Elk Mountain. *J. Geoph. Res.*, **83,** 5050–5056.

Schmidt, R. A., Jr., 1972: Sublimation of wind-transported snow—a model. USDA Forest Serv. Res. Pap. RM-90, Rocky Mountain Forest and Range Experiment Station, Fort Collins, 24 pp.

——, 1981: Estimates of threshold wind speed from particle sizes in blowing snow. *Cold Regions Sci. Techn.*, **4,** 187–193.

——, 1982: Properties of blowing snow. *Rev. Geophys. Space Phys.*, **20,** 39–44.

Vali, G., M. K. Politovich and D. G. Baumgardner, 1981: Conduct of cloud spectra measurements. Report AFGL-TR-81-0122, Air Force Geoph. Lab., Available from Nat'l. Techn. Inf. Serv., Order No. AD-A102944/6.

——, D. C. Rogers and T. L. Deshler, 1982: Ice nucleus and ice crystal measurements in cap clouds. *Proc. Amer. Meteor. Soc. Conf. Cloud Physics,* Chicago, 333–334.

Vardiman, L., 1978: The generation of secondary ice particles in clouds by crystal-crystal collisions. *J. Atmos. Sci.*, **35,** 2168–2180.